Virology 538 (2019) 97–110

Contents lists available at ScienceDirect

Virology

journal homepage: www.elsevier.com/locate/virology

END-phenomenon negative bovine viral diarrhea virus that induces the host's innate immune response supports propagation of BVDVs with different immunological properties

Mai Shiokawa[a], Tsutomu Omatsu[b], Yukie Katayama[b], Kaoru Nishine[a,c], Yuri Fujimoto[d,1], Shiori Uchiyama[a], Ken-ichiro Kameyama[e], Makoto Nagai[b], Tetsuya Mizutani[b], Yoshihiro Sakoda[d], Akio Fukusho[a], Hiroshi Aoki[a,*]

[a] School of Veterinary Nursing and Technology, Faculty of Veterinary Science, Nippon Veterinary and Life Science University, Tokyo, Japan
[b] Research and Education Center for Prevention of Global Infectious Disease of Animal, Faculty of Agriculture, Tokyo University of Agriculture and Technology, Tokyo, Japan
[c] Kyoto Biken Laboratories, Inc. Formulation Department, Formulation Section 1, Kyoto, Japan
[d] Laboratory of Microbiology, Department of Disease Control, Faculty of Veterinary Medicine, Hokkaido University, Hokkaido, Japan
[e] Division of Transboundary Animal Disease, National Institute of Animal Health, NARO, Ibaraki, Japan

ARTICLE INFO

Keywords:
BVDV
END-Phenomenon
Co-infection

ABSTRACT

Our previous study reported that persistently infected (PI) cattle of bovine viral diarrhea virus (BVDV) have co-infected with BVDV/END$^-$ and /END$^+$ that promote and inhibit host's type-I interferon (IFN) production, respectively. However, the relationship between co-infection of immunologically distinct BVDVs and persistent infection as well as the biological significance of END$^-$ viruses remains unknown. Experiments using cultured cells revealed that END$^+$ virus, which is unable to propagate in situations where the host's immune response is induced by IFN-α addition, is able to propagate under those conditions when co-infecting with END$^-$ virus. These results indicate that BVDV/END$^-$ can coexist with BVDV/END$^+$ and that co-infection with END$^-$ viruses supports the propagation of END$^+$ viruses. Our *in vitro* experiments strongly suggest that co-infection with END$^-$ virus is involved in the maintenance of persistent infection of BVDV.

1. Introduction

Bovine viral diarrhea virus (BVDV) is an enveloped, positive-stranded RNA virus (genus, *Pestivirus*; family, *Flaviviridae*). BVDV infection incurs crucial economic losses for cattle producers worldwide (Fourichon et al., 2005; Richter et al., 2017). In general, acute BVDV infections cause transient fever and diarrhea, nasal discharge, and reduced milk yield, and animals recover from these infections by mounting their own immune response. However, clinical symptoms of infected cattle are diverse, varying from subclinical to severe. Furthermore, transplacental infection with BVDV can lead to spontaneous abortions, fetal abnormalities, or the birth of persistently infected (PI) calves. Although they exhibit only few clinical symptoms, PI calves excrete large amounts of viruses throughout their lives and hence become a chronic source of BVDV infection in cattle farms. Furthermore, PI calves are at risk of developing fatal mucosal disease (MD) (Lanyon et al., 2014).

Several studies have reported on the innate immune regulatory mechanisms of both BVDV and classical swine fever virus (CSFV), also a member of the genus *Pestivirus*. These studies indicated that the proteins N^{pro} and E^{rns} of BVDV and CSFV play important roles as interferon (IFN) antagonists (Gottipati et al., 2016; Mine et al., 2015; Tamura et al., 2014; Magkouras et al., 2008; Seago et al., 2007). Other previous reports have indicated that the protein N^{pro} can block dsRNA-induced apoptosis and induce proteasomal degradation of interferon regulatory factor-3 in infected cells. This function of N^{pro} causes transcriptional inhibition of IFN-β production, leading to suppression of host innate immune responses (Baigent et al., 2002; Ruggli et al., 2003; Hilton et al., 2006). Because pestivirus N^{pro} is nonessential for viral replication (Tratschin et al., 1998), its functions may be specialized to suppress the

* Corresponding author. School of Veterinary Nursing and Technology, Faculty of Veterinary Science, Nippon Veterinary and Life Science University, 1-7-1, Kyonancho, Musashino, Tokyo, 180-8602, Japan.
E-mail address: aokihir@nvlu.ac.jp (H. Aoki).
[1] Present address: Veterinary Epidemiology Unit, Graduate School of Veterinary Medicine, RakunoGakuen University, Hokkaido, Japan.

https://doi.org/10.1016/j.virol.2019.09.016
Received 5 September 2019; Received in revised form 30 September 2019; Accepted 30 September 2019
Available online 02 October 2019
0042-6822/

host innate immune response. The pestivirus E^{rns} protein has RNase activity and inhibits viral ssRNA- and dsRNA-induced IFN production; further, its inhibitory activity persists for several days, indicating it is a potent IFN antagonist with an activity comparable with that of N^{pro} (Zurcher et al., 2014). Furthermore, the functions of N^{pro} and E^{rns} are necessary for the establishment of persistent fetal infection (Meyers et al., 2007). Therefore, N^{pro} and E^{rns} are thought to be key mediators of innate immune evasion and persistent infection establishment (Peterhans and Schweizer, 2013). The immunosuppressive function of N^{pro} and E^{rns} alone may not be enough to explain the immune response to BVDV infection. The immune response to BVDV infection *in vivo* and *in vitro* has been reported to differ depending on the type of infected cells and the infection pattern (i.e., acute or persistent infection) (Brackenbury et al., 2005; Reid et al., 2016; Yamane et al., 2008; Van Wyk et al., 2016). BVDV may have the complex immune regulatory system in a way that cannot be explained by N^{pro} and E^{rns} functions. The changes in host immune response are thought to be involved in the onset of various symptoms as well as in the maintenance of persistent infections in BVDV-infected animals.

BVDV is classified into the cytopathogenic (cp) and non-cytopathogenic (ncp) biotypes based on morphological changes in virus-infected cultured cells (Zhang et al., 1996). Most field strains are ncpBVDVs, and only ncpBVDVs can establish persistent infections (Harding et al., 2002). Both cp and ncp viruses can be isolated from animals that have developed MD. Therefore, the presence of cpBVDV in a PI animal is believed to be closely related to the progression to MD (Brownlie, 1990). In addition, ncpBVDV and CSFV can be further divided into two virus types (Table 1). The first type exhibits a phenotype known as the exaltation of Newcastle disease virus (NDV) phenomenon (END^+) (Inaba et al., 1963, 1968; Kumagai et al., 1958). The second type does not have this phenotype (END^-). END^- viruses interfere with superinfection by vesicular stomatitis virus (VSV) and western equine encephalitis virus (Fukusho et al., 1976; Itoh et al., 1984; Nakamura et al., 1993; Shimizu et al., 1970). Nakamura et al. (1993, 1995) reported that these two BVDVs, END^+ and END^-, were isolated from several BVDV strains such as NADL, Osloss, New York-1, No.12-43, Indiana-46, Nose, and KS86. Previous reports have indicated that END^- and END^+ viruses exhibit different immunological properties. In particular, END^- and END^+ viruses induce and inhibit the production of type-I IFN in infected cells, respectively (Kozasa et al., 2015). END^+ and END^- viruses can be separately harvested either using cloning methods after limiting dilution (based on the END-phenomenon) or using reverse plaque formation (RPF) based on interference with VSV (Inaba et al., 1963; Fukusho et al., 1976). Although these methods have not yet been confirmed to yield viruses with homogeneous genetic properties, they allow for the separation of viruses that share similar immunological properties.

GPE^-, an END^- virus isolated from virulent CSFV ALD strain, has been used as an attenuated vaccine strain and has greatly contributed to the eradication of CSFV in Japan in past. The ability of END^- viruses to strongly induce host immune responses makes it suitable for use as a vaccine strain but renders such viruses difficult to propagate. Therefore, the biological significance of END^- viruses remains largely unknown. Our previous study revealed not only that BVDV/ END^- are widely distributed in the field of Japan, but also that both END^+ and END^- virus have been co-infected at various ratios in PI cattle (Nishine et al., 2014). Co-infection with these BVDVs may contribute to the development of disease, onset of MD, and maintenance of persistent infection.

The present study aimed at clarifying the biological significance of END^- viruses and investigating their association with co-infection with immunologically distinct BVDVs. BVDV can reportedly lead to persistent infection even in *in vitro* experiments (using cultured cells) (Durantel et al., 2004); hence, MDBK cells were co-infected with immunologically distinct BVDVs under various conditions, and the resulting viruses were subjected to repeated passaging. Even when the END^+ virus was the dominantly propagating type, the END^- virus was observed to be continuously produced in the culture supernatant. Furthermore, contrary to the END^- virus, it was also reveal that the END^+ virus was unable to propagate in the presence of IFN-α. However, we observed that END^+ virus was able to propagate even in the presence of IFN-α if the END^+ virus is co-infected with END^- virus. Thus, co-infection with the END^- virus helped the END^+ virus propagation even in the presence of potent host innate immune responses, suggesting that co-infection contributes to the evasion of host immunity and maintenance of persistent infection *in vivo*. Thus, the END^- virus, which is also detected in PI cattle, may play an important role in maintaining persistent infection *in vivo* by supporting the growth of BVDV with different immunological properties.

2. Results

2.1. Production of infectious vBVD12$^-$ and vBVD12$^-$/P8L particles

Previous studies using the NADL strain of cpBVDV reported that a Leu8Pro mutation in N^{pro} resulted in dramatic changes in the innate immune response induced by viral infection (Gil et al., 2006). The proteins encoded by END^- (accession no. LC068605) and END^+ (accession no. LC068604) ncpBVDVs of the No. 12 strain differ at only five amino acid positions (one of these is at position 8 in N^{pro}, which is a Pro in the END^- virus and a Leu in the END^+ virus). Therefore, we focused on the potential roles of N^{pro} in innate immune response and constructed a mutant of the END^- virus encoding an N^{pro} protein harboring a Pro8Leu substitution. The resulting mutant virus was designated vBVD12$^-$/P8L and its properties were analyzed.

First, individual RNAs transcribed from the linearized plasmids pBVD12$^-$ and pBVD12$^-$/P8L encompassing the cDNA sequences of the respective BVDVs were introduced into MDBK cells by electroporation.

Table 1
Properties of BVDV and CSFV phenotypes.

Virus		Note	END–phenomenon	VSV interference	Reference
CSFV	GP	attenuated to guinea pig cells (avirulence)			
	GPE+	cloned from GP	Positive[a]	Negative	Kumagai et al. (1958)
	GPE−	cloned from GP	Negative[b]	Positive	Fukusho et al. (1975)
	ALD	cloned from field strain (high virulence)			
	ALD-E−	cloned from ALD	Negative	Positive	Aoki et al. (2004)
BVDV	No.12	cloned from field strain			
	vBVD12–	generated by reverse genetics in this study	Negative	Positive	
	vBVD12–/P8L	generated by reverse genetics in this study	Positive	Negative	

[a] END–phenomenon positive virus which dose not interfere with VSV is called END+.
[b] END–phenomenon negative virus which interferes with VSV is called END–.

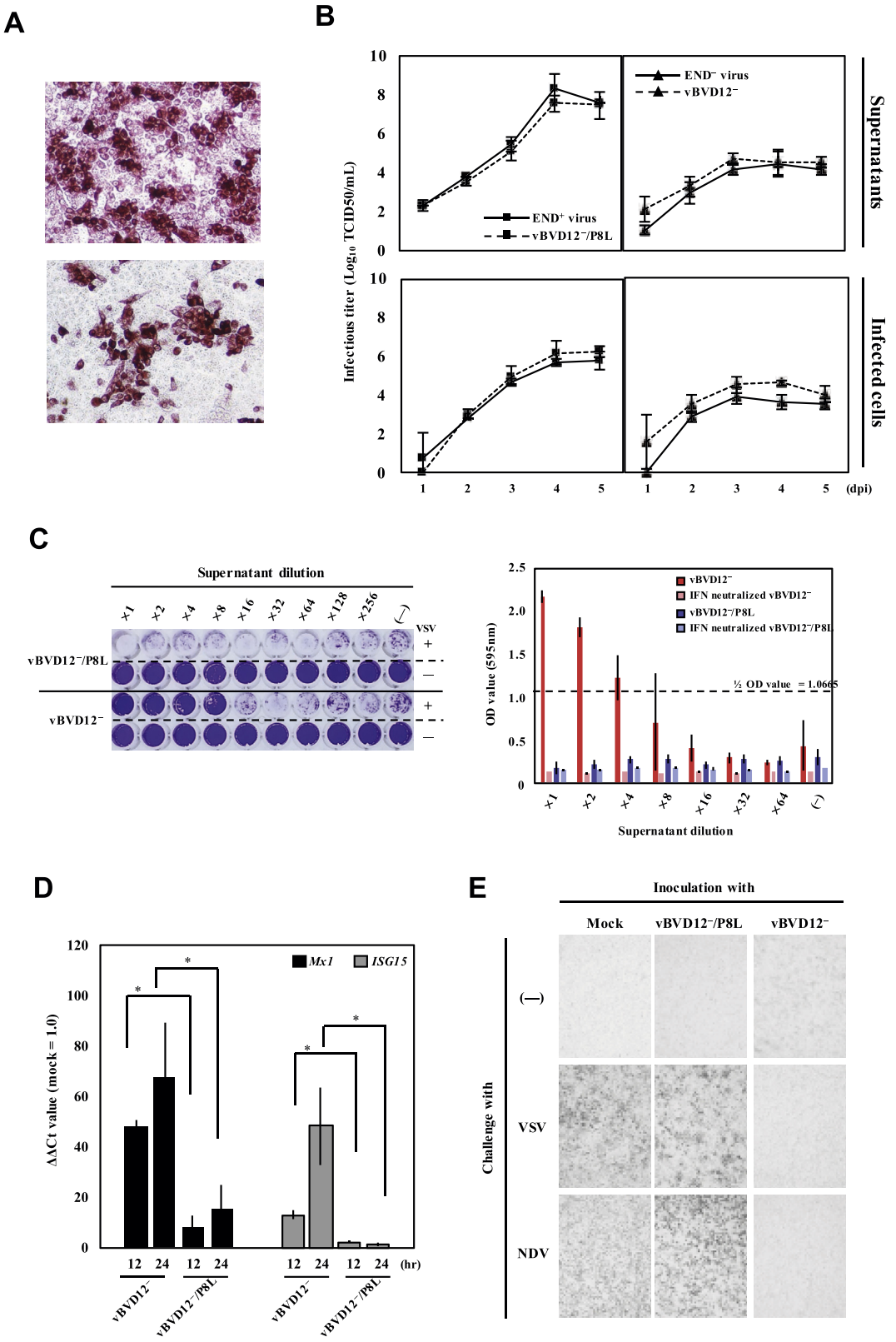

(caption on next page)

Three days after electroporation, a peroxidase-linked assay (PLA) was used to confirm whether BVDV-positive cells were present. Although BVDV-positive cells were present in almost all MDBK cell cultures carrying RNA of BVD12^{-}/P8L (Fig. 1A, upper panel), BVDV-positive cells formed a small focus in MDBK cells carrying RNA of BVD12^{-} (Fig. 1A, lower panel). The distribution of BVDV-positive cells may depend on the innate immune response induced by the produced virions. The culture supernatant was also collected from each RNA-transfected MDBK cells at 3 days after electroporation (P.0 virus). To compare growth kinetics, naïve MDBK cells were infected with parental

Fig. 1. Characterization of vBVD12$^-$ and vBVD12$^-$/P8L
(A) The distribution of BVDV-positive cells was assessed using PLA 3 days after electroporation of pBVD12$^-$/P8L (top panel) or pBVD12$^-$ (bottom panel) viral RNA. (B) Naïve MDBK cells were infected with P.0 virus (vBVD12$^-$ and vBVD12$^-$/P8L) and parental virus (END$^-$ virus and END$^+$ virus) at an MOI of 0.01, and the culture supernatants and infected cells were harvested at 1–5 dpi. Four freeze–thaw cycles were used to prepare infectious particles from the infected cells. The upper panels indicate the total BVDV titer in the supernatant, whereas the lower panels indicate the titer in the infected cells. The total BVDV titer was measured thrice using PLA. (C) The supernatant recovered from vBVD12$^-$- and vBVD12$^-$/P8L-infected cells was filtered to eliminate viral particles and then used for the IFN bioassay. These supernatants were used to sensitize naïve MDBK cells for 24 h, and the cells were then challenged with VSV. Twenty-four hours after VSV challenge, the cells were stained with 0.25% crystal violet (left panel). The OD value was measured and compared for vBVD12$^-$ and vBVD12$^-$/P8L. Each viral fluid after filtration was also neutralized with an anti-IFN antibody and analyzed (right panel). (D) MDBK cells were infected with vBVD12$^-$ or vBVD12$^-$/P8L, and intracellular *Mx1* and *ISG15* mRNA were quantified using qRT-PCR. Asterisks indicate significant differences ($P < 0.05$). (E) The biological properties of viruses produced in this study were examined using END and VSV-interference assays.

virus or P.0 virus at a multiplicity of infection (MOI) of 0.01. The vBVD12$^-$ and vBVD12$^-$/P8L viruses showed similar growth kinetics as the parent virus, and the viral titers obtained 5 days post-infection (dpi) were nearly equivalent (Fig. 1B, upper panels). The titers of infectious viruses within the vBVD12$^-$- and vBVD12$^-$/P8L-infected cells were slightly higher than those of cells infected with the parent virus; however, the growth kinetics was nearly identical (Fig. 1B, lower panels). In both the culture supernatants and infected cells at 5 dpi, vBVD12$^-$/P8L showed approximately 100-fold higher viral titers than vBVD12$^-$ ($P < 0.05$).

Next, to investigate the immunological characteristics of these viruses, an IFN bioassay was performed to determine whether type-I IFN was produced in culture supernatants following infection by either virus. Prior to the assay, supernatants were filtered to eliminate viral particles. MDBK cells sensitized with filtered supernatants of vBVD12$^-$-infected cells inhibited the cytopathic effect (CPE) upon VSV superinfection; in contrast, the filtered supernatants of vBVD12$^-$/P8L-infected cells did not inhibit CPE (Fig. 1C, left panel). Measurement of optical density (OD) values indicated that the supernatant of cells infected with vBVD12$^-$ contained sufficient IFN-α and IFN-β to inhibit 50% of the CPE induced by VSV infection even when diluted four-fold. In contrast, the supernatant of vBVD12$^-$/P8L-infected cells showed that no detectable levels of type-I IFN were produced. To confirm whether the factor inhibiting CPE by VSV infection was actually type-I IFN, neutralization of type-I IFN was also performed for each filtered fluid. The OD values of vBVD12$^-$ supernatants considerably decreased upon IFN neutralization; this confirmed that the supernatant derived from vBVD12$^-$-infected cells contained type-I IFN (Fig. 1C, right panel). These results suggested that the two BVDVs produced in this study exhibited different immunological properties. To address this observation, the abundance of *Mx1* and *ISG15* mRNAs in infected cells was measured by quantitative reverse-transcription PCR (qRT-PCR). As expected, expression of both mRNAs was significantly higher in vBVD12$^-$-infected cells; however, no significant increase was observed in the vBVD12$^-$/P8L-infected cells compared with mock-infected cells (Fig. 1D). To confirm the biological types of both viruses, END and VSV-interference assays were performed. In cells infected with vBVD12$^-$/P8L, enhancement of CPE upon NDV superinfection was observed; however, CPE upon VSV superinfection was not inhibited. In contrast, vBVD12$^-$-infected cells completely blocked the CPEs induced by both VSV and NDV superinfection (Fig. 1E). These results revealed that vBVD12$^-$/P8L and vBVD12$^-$ exhibited the same biological properties as END$^+$ and END$^-$ viruses (Table 1), respectively, demonstrating successful production of these each BVDV with distinct immunological properties using reverse genetics techniques.

2.2. vBVD12$^-$/P8L was dominantly propagated during co-infection with vBVD12$^-$ in vitro

To investigate the kinetics of infection with vBVD12$^-$ and vBVD12$^-$/P8L, MDBK cells were infected with each virus at an MOI of 1.0 (Fig. 2) and the culture supernatants were passaged 10 times (P.10). We found that vBVD12$^-$/P8L was propagated at a higher viral titer than vBVD12$^-$ (Fig. 2, left and middle panels). We hypothesized that this difference in infectious kinetics was due to the innate immune response induced by infection with the respective viruses. Because vBVD12$^-$ induces type-I IFN production in infected cells, the viral titer was expected to decrease as passaging was repeated. However, vBVD12$^-$ titers were not eliminated by immune responses elicited by own infection and maintained its propagation (Fig. 2, left panel). A recent publication reported that both BVDVs were detected in PI cattle in the field (Nishine et al., 2014), and it was suggested the possibility that these BVDVs were co-infected in PI cattle. Therefore, to examine the influence of co-infection by immunologically contrasting BVDVs, MDBK cells were co-infected by adjusting the MOI of each virus to 1.0, and the culture supernatant was passaged 10 times. The total BVDV titer varied between $10^{5.88\text{-}7.8}$ 50% tissue culture infectious dose (TCID50)/mL, indicating stable growth kinetics (Fig. 2, right panel).

To determine which virus types were predominantly propagated during co-infection, we analyzed the innate immune response occurring in infected cells and virus titration using a biological method. END and VSV-interference assays were performed to determine the dominant virus type present in the P.10 supernatant. Upon infection with the P.10 supernatant, MDBK cells exhibited the END-phenomenon; the infected cells showed enhancement of CPE upon NDV superinfection and did not block CPE upon VSV superinfection (Fig. 3A). Therefore, it appeared that vBVD12$^-$/P8L was the dominant in the P.10 supernatant. IFN bioassays also were performed, and the results indicated that MDBK cells treated with each filtered supernatant (P.1, P.3, P.5, P.7, and P.10) obtained from co-infected cells failed to block the CPE induced by VSV superinfection. Moreover, the measured OD values were approximately equal to those obtained from cells exposed to the filtered supernatant of vBVD12$^-$/P8L-infected cells (Fig. 3B). It was found that type-I IFN was not detected in culture supernatant during co-infection. In addition, in cells infected with the P.1, P.3, P.5, P.7, and P.10 supernatant, neither intracellular *Mx1* nor *ISG15* mRNA expression was detected (Fig. 3C). These results revealed that an innate immune response in infected cells was not elicited during co-infection and that vBVD12$^-$/P8L propagates in a dominant fashion over vBVD12$^-$ during co-infection. Therefore, we tried to measure the titer of vBVD12$^-$/P8L by END assay using limiting dilution. Consistently, vBVD12$^-$/P8L exhibited a titer comparable with the total BVDV titer, albeit a difference was observed between the vBVD12$^-$/P8L and total BVDV titers (Fig. 3D).

2.3. END$^-$ virus continued to be produced during co-infection

The results shown in Fig. 3 indicate that the END$^+$ virus was propagated as the dominant virus type during co-infection with the END$^-$ virus; however, these data do not prove that the END$^-$ virus was not propagating. In addition, based on data presented in Fig. 3D, there was a difference between the END$^+$ and total BVDV titers, which suggested the possibility that the END$^-$ virus was present in the supernatant. To confirm the presence of the END$^-$ virus, we attempted to detect vBVD12$^-$ in the supernatant by performing PCR using HiDi DNA polymerase and the RPF method. First, we confirmed whether the HiDi DNA polymerase could be used to discriminate viruses differing by a single nucleotide. Because vBVD12$^-$ and vBVD12$^-$/P8L differ at a single nucleotide (position No.410) in the genomic region encoding

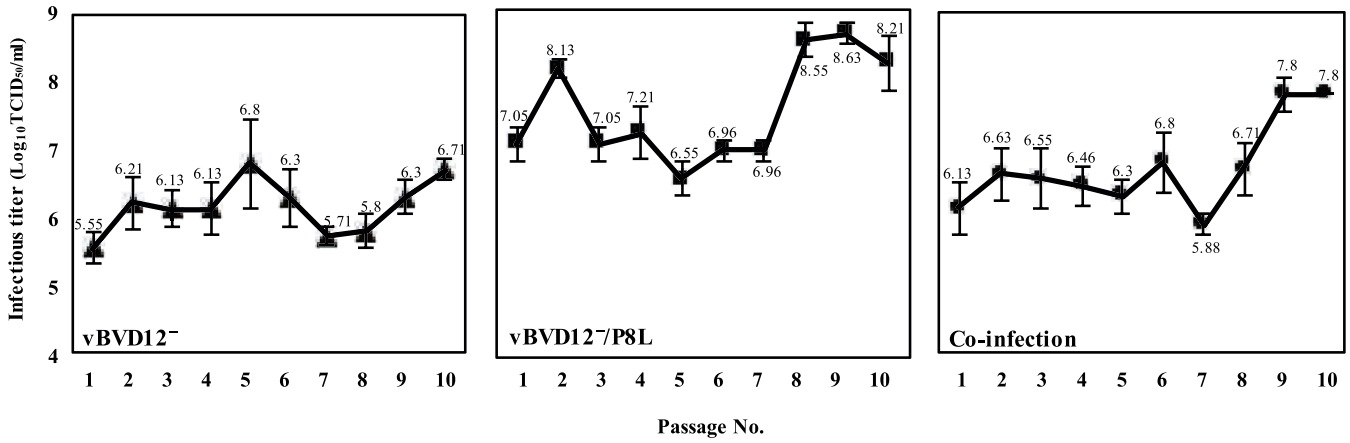

Fig. 2. Viral growth kinetics during single- and co-infection
In single-infection studies, MDBK cells were infected with either vBVD12$^-$ (left panel) or vBVD12$^-$/P8L (middle panel) at an MOI of 1.0. In co-infection studies, MDBK cells were infected with both vBVD12$^-$ and vBVD12$^-$/P8L (together) at an MOI of 1.0 (right panel). The supernatant was collected 4 days after the viral infection, and the supernatant was passaged until the P.10 supernatant was obtained. The total BVDV titer was quantified thrice using PLA.

N^{pro}, this mutation was designed to be located at the 3' end of each forward primer for PCR. RNA was extracted from viruses generated through reverse genetics, and cDNA was synthesized and used as the template for PCR. This pilot experiment confirmed that the primers designed for the detection of vBVD12$^-$ yielded amplicons specifically from vBVD12$^-$, whereas the primer designed for the detection of vBVD12$^-$/P8L yielded amplicons specifically from vBVD12$^-$/P8L (Fig. 4A). Next, we attempted detection of each viral gene from supernatants harvested from co-infected cells. We found that all the supernatant samples yielded amplicons corresponding to both vBVD12$^-$/P8L and vBVD12$^-$ (Fig. 4B). However, the detection of the viral genes did not prove the presence of infectious vBVD12$^-$ particles. Therefore, we attempted to detect infectious vBVD12$^-$ particles from the supernatants of P.1, P.5, and P.10 using the RPF assay. Reverse plaques representing vBVD12$^-$ infection were detected in each of these samples (Fig. 4C), indicating that vBVD12$^-$ continued to be produced in the culture supernatant even when vBVD12$^-$/P8L was dominant propagated during co-infection. The viral titer measured using the RPF method was approximately $10^{4.36\text{-}5.42}$ TCID50/mL (Fig. 4D). Even when vBVD12$^-$/P8L predominated, vBVD12$^-$ was still present in the supernatant, indicating the END$^-$ virus could coexist with END$^+$ virus.

2.4. END$^-$ and END$^+$ viruses showed different sensitivities to IFN-α

To clarify the reason why the END$^-$ virus coexisted with END$^+$ virus, the properties of the END$^-$ virus were examined in further detail. To know how host innate immune responses affect the growth of the END$^-$ virus, vBVD12$^-$ was passaged in the presence of IFN-α and viral growth kinetics were examined. A previous study showed that human IFN-α is also active in bovine cells (Peek et al., 2004); hence, human recombinant IFN-α was used in this study. Supernatants of viral passages from P.1 to P.7 were supplemented with 3 ng IFN-α per 25-cm^2 flask; however, no significant effects on viral propagation were observed. Therefore, the passages after P.7 were performed in the presence of IFN-α at a concentration of 30 ng/flask. As assessed by PLA, the viral titer of vBVD12$^-$ was reduced at P.11, after which vBVD12$^-$ persisted at a titer of approximately $10^{5.0}$ TCID50/mL (Fig. 5A). Thus, we concluded that the END$^-$ virus was able to propagate even in the presence of IFN-α, simulating host innate immune responses. To determine the characteristics of repeatedly passaged virus in the presence of IFN-α, the immunological characteristics of the P.25 virus were evaluated. Of note, cells infected with the P.25 virus exhibited inhibition of VSV and NDV superinfection at levels similar to those seen in cells infected with P.0 of vBVD12$^-$ (Fig. 5B). In addition, IFN-neutralized P.25 virus also showed inhibition of CPE upon VSV and NDV superinfection (data not shown). These results indicated that the P.25 virus induced type-I IFN production in the culture supernatant through its own infection and that the amount of IFN produced was sufficient to inhibit VSV and NDV superinfection. Moreover, the expression of *Mx1* and *ISG15* mRNAs considerably increased in P.25-infected cells compared with mock-infected cells (Fig. 5C). Upregulation of these mRNAs was also observed when the experiment was conducted using IFN-neutralized P.25 virus (data not shown). Using IFN bioassay, we also confirmed that type-I IFN was produced in the supernatant of cells infected with P.25 virus. The OD value decreased upon IFN neutralization, confirming that the culture supernatant of P.25-infected cells contained type-I IFN (Fig. 5D). These results revealed that the P.25 virus retained its ability to enhance host innate immunity and showed the same biological properties as P.0 of vBVD12$^-$. In addition, the susceptibility of vBVD12$^-$/P8L to IFN-α was examined, and we observed that vBVD12$^-$/P8L did not propagate in the presence of IFN-α (Fig. 5E). These results indicate that during innate immune responses induced *in vitro*, the END$^+$ virus cannot maintain infection. In contrast, the END$^-$ virus can maintain infection under these conditions.

2.5. Co-infection with END$^-$ virus allowed propagation of END$^+$ virus in situations where host innate immune responses were activated

PI cattle are reportedly co-infected with immunologically distinct BVDVs (Nishine et al., 2014); however, the implications of this co-infection have not yet been clarified. We found that these BVDVs exhibited different sensitivities to IFN-α (Fig. 5A and E). Therefore, we hypothesized that BVDV may maintain their infection by changing the type of virus that propagates according to the host innate immune response. To test this hypothesis, supernatant obtained from co-infected cells was passaged in either the presence or absence of IFN-α until P. 25 was obtained. Thereafter, the type of virus contained in the supernatant was determined.

First, we checked the total BVDV titer of all of the resulting supernatants. Between P.1 and P.4 in the absence of IFN-α, the total BVDV titer was high at approximately $10^{7.0}$ TCID50/mL, but gradually decreased with the addition of IFN-α. However, although the titer decreased to $10^{4.96}$ TCID50/mL at P.9, the titer subsequently increased rapidly to $10^{6.88}$ TCID50/mL at P.10. Thereafter, a titer of approximately $10^{6.0}$ TCID50/mL was maintained even in the presence of IFN-α during further passaging. When IFN-α was again removed, the BVDV titer increased even more, reaching $10^{8.3}$ TCID50/mL at P.16. IFN-α was added again after P.20, but no significant decrease in titer was

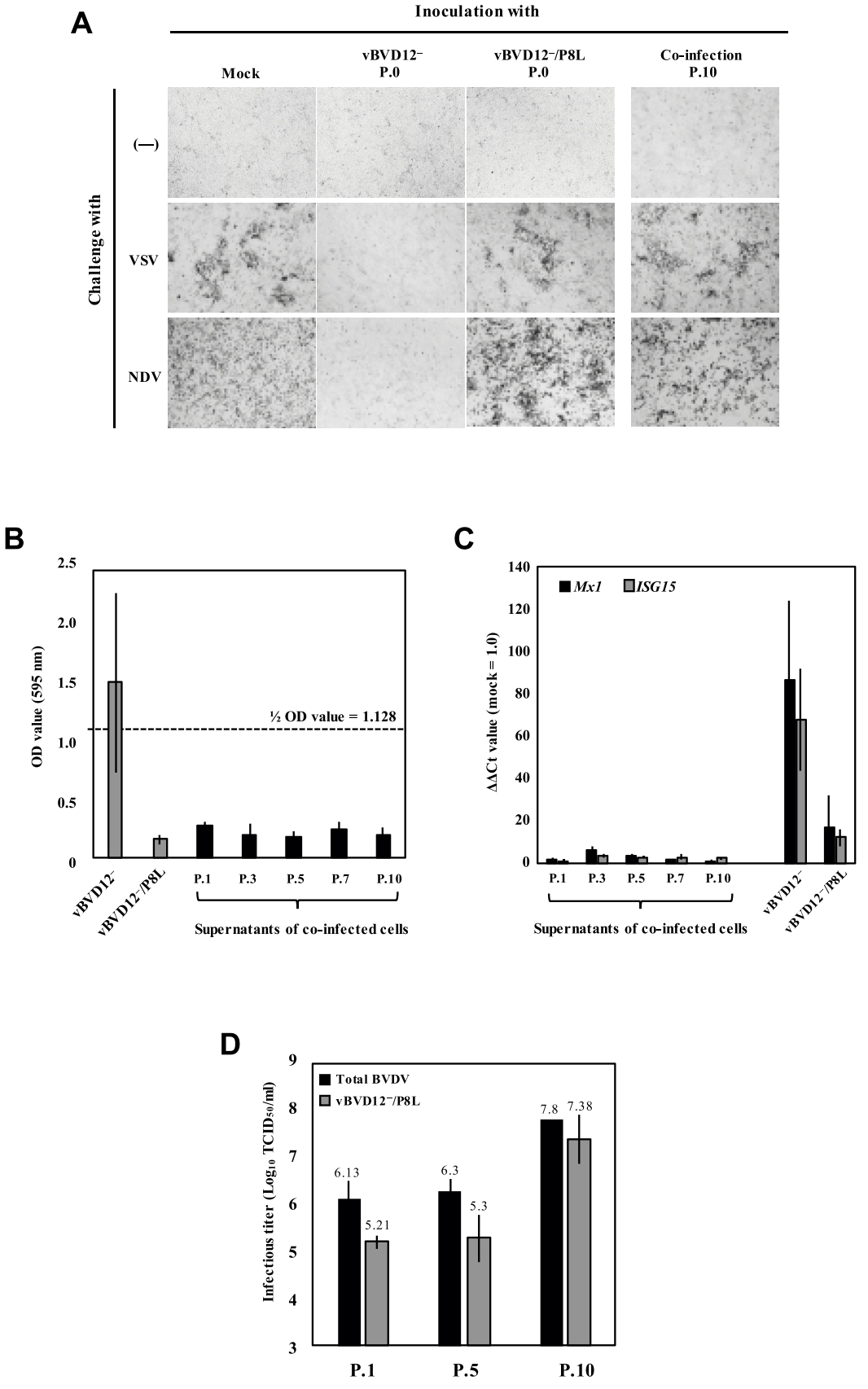

(caption on next page)

Fig. 3. Investigation of the major virus types contained in the supernatant obtained during BVDV co-infection
(A) The major virus types contained in the supernatant of P.10 of co-infected cells was confirmed using END and VSV-interference assay. Viruses obtained from P.0 were used as the positive control. (B) The supernatant samples collected from co-infected cells (P.1, P.3, P.5, P.7, and P.10) were filtered to eliminate viral particles and then used for the IFN bioassay. CPE was confirmed at 24
h after VSV challenge, and the OD value was measured. Filtered supernatants derived from vBVD12$^-$ or vBVD12$^-$/P8L were used as positive controls. (C) MDBK cells were infected with the supernatants of co-infected cells (P.1, P.3, P.5, P.7, and P.10), and the cells were collected at 24 hpi. Intracellular *Mx1* and *ISG15* mRNAs were quantified using qRT-PCR. vBVD12$^-$ or vBVD12$^-$/P8L were used as positive controls. (D) The titers of vBVD12$^-$/P8L contained in the supernatants of P.1, P.5, and P.10 of co-infected cells were measured by limiting the dilution using the END assay (gray bars). The total BVDV titer (black bars) obtained in the PLA shows the results as presented in right panel of Fig. 2.

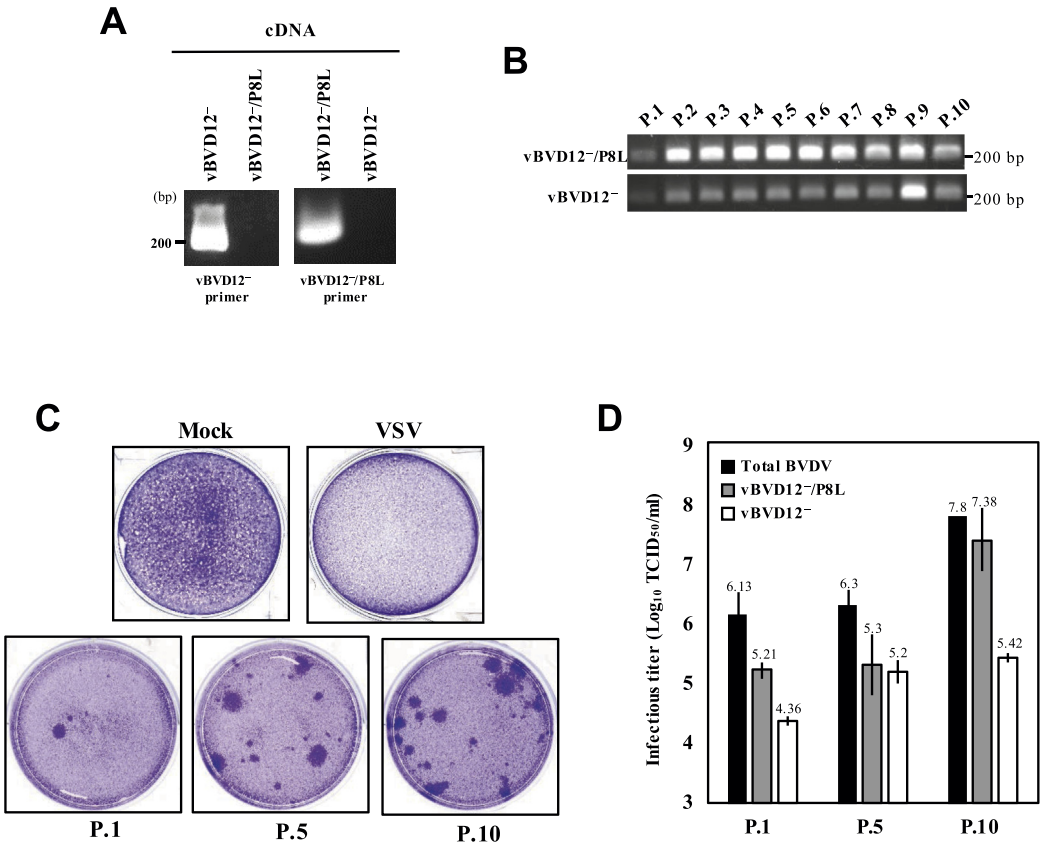

Fig. 4. END$^-$ virus continued to be produced during co-infection *in vitro*
(A) HiDi DNA polymerase could distinguish a single nucleotide difference. The primer designed for the detection of vBVD12$^-$ yielded amplicons only from vBVD12$^-$ (left panel), and the primer designed for the detection of vBVD12$^-$/P8L yielded amplicons only from vBVD12$^-$/P8L (right panel). (B) Viral genes derived from vBVD12$^-$ or vBVD12$^-$/P8L in the supernatant collected from co-infected cells was detected using PCR with HiDi DNA polymerase. (C) Infectious particles of vBVD12$^-$ contained in the supernatant of co-infected cells (P.1, P.5, and P.10) were detected using the RPF assay. The supernatant was diluted 10,000-fold and was used to inoculate BT cells. (D) The titer of vBVD12$^-$ contained in the supernatant of co-infected cells (P.1, P.5, and P.10) was measured using the RPF assay (white bars). Total BVDV (black bars) and vBVD12$^-$/P8L titers (gray bars) can be seen in the results presented in Fig. 3D.

observed (Fig. 6A). To assess the virus types contained in the supernatants, genes encoding the N^{pro}-encoding viral region were detected using PCR with HiDi DNA polymerase. Unexpectedly, the level of vBVD12$^-$ gradually decreased after P.5 and was undetectable in samples other than P.9, P.10, and P.18. Surprisingly, vBVD12$^-$/P8L was continuously detected regardless of the addition of IFN-α (Fig. 6B). We performed deep sequencing analysis using supernatant samples (P.1, 3, 7, 10, 14, 18, 21, and 25) to confirm whether the type of propagating virus changed before and after adding IFN-α. In the P.7, P.10, P.21, and P.25 samples, which were collected from a culture maintained with IFN-α, the nucleotide denoting vBVD12$^-$/P8L (nucleotide No.410:T) accounted for 92.55–98.54% of all nucleotides in position No.410. The proportion of nucleotide "T" gradually increased as the passage was repeated (Table 2). This result showed that vBVD12$^-$/P8L was the major population in the supernatant, even when the innate immune responses were activated by IFN-α addition. The nucleotide denoting vBVD12$^-$ (nucleotide No.410: C) was continuously detected from the supernatants of co-infected cells even when vBVD12$^-$/P8L was the major population. When the consensus sequence of these samples was confirmed, there were no mutations in bases other than that at position No.410 (data not shown). Deep sequencing analysis showed that vBVD12$^-$/P8L is the major virus type in the supernatant regardless of IFN-α addition, so we examined whether the END-phenomenon could be observed using the supernatants of P.3, P.10, 18, and P.25. As a result, enhancement of CPE induced by NDV superinfection was clearly observed in cells infected with each of the filtered supernatants. These samples were found to contain abundant vBVD12$^-$/P8L (Fig. 6C). Furthermore, the RPF assay revealed that vBVD12$^-$ was also produced in these supernatants (Fig. 6D). Although the vBVD12$^-$ titer was lower than that of vBVD12$^-$/P8L, we confirmed that vBVD12$^-$ was reliably produced in the supernatant (Fig. 6E). The results shown in Fig. 5E demonstrated that a single infection with the END$^+$ virus could not be maintained in the presence of host innate immune responses. The data shown in Fig. 6 and Table 2 show that, if cells infected with the END$^+$ virus were co-infected with the END$^-$ virus, the END$^+$ virus could propagate even in the presence of a host innate immune response. Thus, these data strongly suggest that co-infection with BVDV/END$^-$ supports the propagation of BVDV with different biological properties in *in vitro*.

3. Discussion

At least two types of viruses with distinct immunological properties are involved in ncpBVDVs (Nakamura et al., 1993, 1995), and both types co-infect PI cattle in various ratios (Nishine et al., 2014). Here, we artificially produced immunologically distinct BVDVs (vBVD12$^-$ and vBVD12$^-$/P8L). MDBK cells were co-infected with these viruses under various conditions, and viral growth kinetics and host immune response

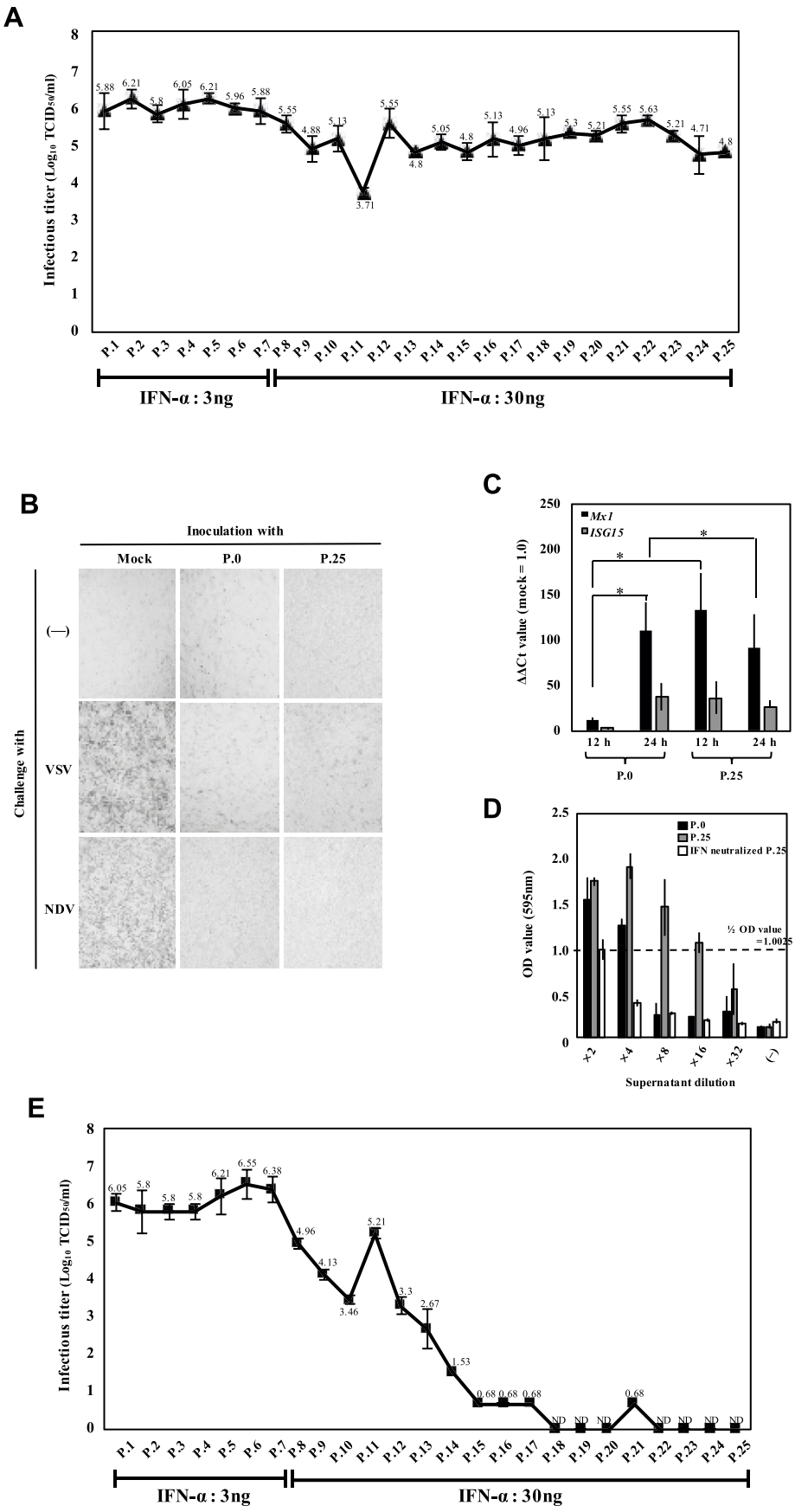

Fig. 5. Susceptibility of vBVD12$^-$ and vBVD12$^-$/P8L to IFN-α and characterization of repeatedly passaged virus (P.25) in the presence of IFN-α

(A) Naïve MDBK cells were infected with vBVD12$^-$ at an MOI of 0.1, and IFN-α was added to the supernatant. IFN-α (3 and 30 ng/flask) was added from P.1 to P.7 and from P.8 to P.25, respectively. The total BVDV titers of all supernatant samples were measured using PLA. (B) The biological properties of the P.25 virus were confirmed using the END and VSV-interference assays. IFN-α contained in the supernatant was filtered prior to the assay. (C) MDBK cells were infected with P.0 of vBVD12$^-$ or the P.25 virus, and cells were collected at 12 and 24 hpi. Intracellular *Mx1* and *ISG15* mRNAs were quantified using qRT-PCR. Asterisks indicate significant differences ($P < 0.05$). (D) The supernatant collected from the P.25 virus-infected cells (gray bars) was filtered to eliminate the viral particles and used for the IFN bioassay. In addition, the P.25 viral fluid after filtration was also treated with the anti-IFN antibody and analyzed (white bars). Filtered supernatants of P.0 vBVD12$^-$-infected cells (black bars) were used as the positive control. (E) vBVD12$^-$/P8L was passaged in the presence of IFN-α. The passage method and the IFN-α addition regimen were the same as described in (A). The total BVDV titers of all supernatant samples were measured using PLA.ND, not detected.

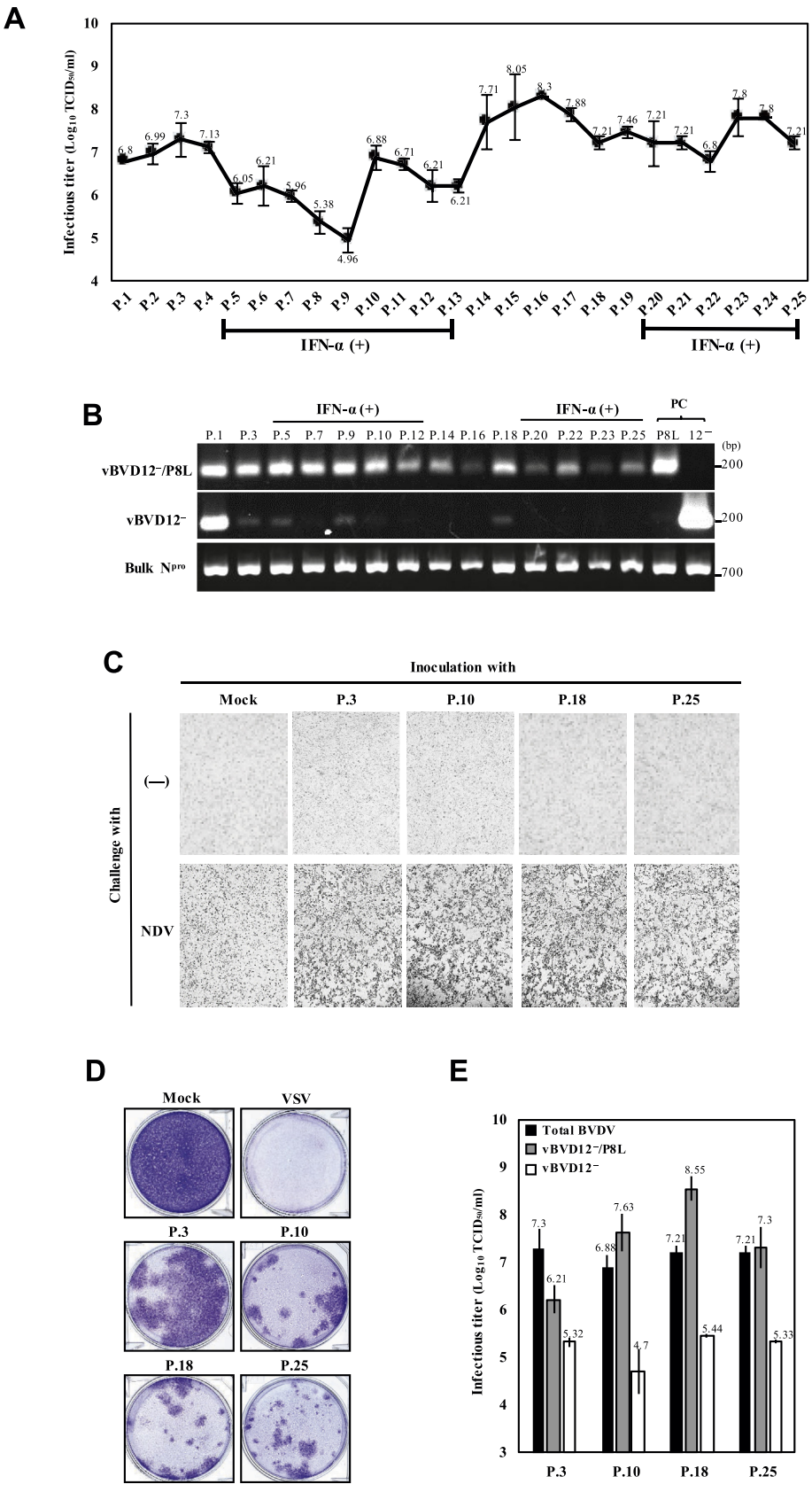

Fig. 6. Co-infection with END$^-$ virus allows END$^+$ virus to propagate even in the presence of IFN-α

(A) MDBK cells were infected with both vBVD12$^-$ and vBVD12$^-$/P8L at an MOI of 0.1, and the supernatant was passaged until P.25 was reached. IFN-α was added from P.5 to P.13 and from P.20 to P.25 but not from P.1 to P.4 and from P.14 to P.19. The concentration of IFN-α added was 30 ng/flask. The total BVDV titers of all supernatant samples were measured using PLA. (B) Each viral gene was detected from the supernatants using PCR with HiDi DNA polymerase. cDNA derived from vBVD12$^-$/P8L (P8L) or vBVD12$^-$ (12$^-$) was used as the positive control. Bulk N^{pro} was detected using conventional PCR, irrespective of the single base mutation in N^{pro}. (C) The biological properties of viruses contained in the P.3, P.10, P.18, and P.25 supernatants were confirmed using the END assay. The supernatant samples were filtered to eliminate IFN-α. (D) Infectious particles of vBVD12$^-$ could be detected in the P.3, P.10, P.18, and P.25 supernatants using the RPF assay. The supernatant samples were diluted 10,000-fold and used to inoculate BT cells. (E) The titers of total BVDV (black bars), vBVD12$^-$/P8L (gray bars), and vBVD12$^-$ (white bars) were measured using PLA, the END assay, and RPF assay, respectively.

changes during co-infection were assessed. Co-infection with END$^-$ virus was observed to support the propagation of END$^+$ virus in the presence of a host innate immune response. Thus, the END$^-$ virus may play an important role in maintaining persistent infection of BVDV, not only *in vitro* but also *in vivo*.

Previous studies employing the NADL strain of cpBVDV have reported that the residue at position 8 of N^{pro} is greatly involved in innate immune regulation (Gil et al., 2006). The vBVD12$^-$/P8L constructed in

Table 2
Proportion of nucleotide at the position No.410 in N^{pro} of generated contigs.

sample	IFN addition	Total read counts	BVDV < read conts	Depth of position No.410	Position No.410 (%)			
					T	C	A	G
P.0 (vBVD12$^-$)		10,85,374	2,77,904	2803	0.14	99.71	0.14	0.00
P.0 (vBVD12$^-$/P8L)		18,89,560	8,49,362	7233	99.00	0.90	0.03	0.07
P.1	–	35,51,596	16,69,138	21,556	80.82	18.94	0.12	0.12
P.3	–	11,15,312	6,31,127	6113	84.10	15.74	0.03	0.13
P.7	+	29,79,156	1,13,269	1531	92.55	6.92	0.39	0.13
P.10	+	13,59,010	3,93,232	4287	96.34	3.48	0.02	0.16
P.14	–	31,28,852	9,15,648	11,358	96.99	2.60	0.19	0.22
P.18	–	30,39,096	4,84,335	5261	97.68	2.07	0.10	0.15
P.21	+	35,75,050	2,02,296	2505	98.28	1.40	0.04	0.28
P.25	+	27,44,856	5,05,269	6855	98.54	1.20	0.06	0.20

the present study suppressed the innate immune response in infected cells, resulting in a dramatic changes in the immune response of vBVD12$^-$ (Fig. 1C–E). Our results indicated that the residue at position 8 of N^{pro} participates in innate immune regulation even in No.12 strain ncpBVDV; other amino acid differences were not required for induction of innate immune response by viral infection.

Although several studies have examined the relationship between BVDV infection and host innate immune responses, no unified view of the innate immune reactions caused by ncpBVDV infection is available (Van Wyk et al., 2016; Charleston et al., 2001; Schweizer and Peterhans, 2001). This confusion may indicate that nominally “pure” laboratory BVDV strains are actually a mixture of BVDVs with different immunological properties. Because biologically distinct BVDVs are present in ncpBVDV in varying ratios, it is difficult to generalize the innate immune response induced by ncpBVDV infection. Of note, the host innate immune response may vary depending on which virus type is dominating during propagation.

The results presented in Fig. 4 suggest that the END$^-$ virus can coexist with END$^+$ virus; however, the role of the END$^-$ virus remains unclear. In addition, co-infection experiments using the END$^+$ and END$^-$ viruses were conducted at MOIs of 1.0 (END$^+$): 0.001 (END$^-$); the experimental results indicated that despite the small amount of initial infectious virus, the END$^-$ virus was also produced in the supernatant (data not shown). These results suggest that the END$^-$ virus plays a role in maintaining persistent infection *in vitro*. Therefore, sensitivity to IFN-α was evaluated to better understand the properties of the END$^-$ virus. The vBVD12$^-$ easily maintained its titer when cultured in the presence of IFN-α; thus, the infection persisted even in the presence of host innate immune response (Fig. 5A). In addition, deep sequencing analysis revealed that the vBVD12$^-$ of P.25 that repeatedly passaged in the presence of IFN-α bore three amino acid mutations in the viral sequence (data not shown). These mutations may help maintain the properties of the END$^-$ virus. In contrast, vBVD12$^-$/P8L, which suppresses host innate immune response, was unable to propagate in the presence of IFN-α (Fig. 5E). Although BVDV can reportedly acquire resistance to type-I IFN (Schweizer et al., 2006), our study revealed that there is at least one BVDV type that cannot acquire IFN-α resistance.

It has been reported that PI cattle have been co-infected with BVDVs having different immunological properties (Nishine et al., 2014) and that innate immune responses are induced even in PI cattle (Shoemaker et al., 2009; Yamane et al., 2008; Smirnova et al., 2012, 2014). Given these previous reports and the results shown in Fig. 5, we hypothesized that BVDV can maintain persistent infection while changing the type of propagating virus based on host innate immune response. To test this hypothesis, we investigated the changes in growth dynamics when host innate immune reaction was induced during co-infection with immunologically distinct BVDVs (resembling the case in PI cattle). However, contrary to our hypothesis, vBVD12$^-$/P8L was found to dominantly propagate when IFN-α was added during co-infection (Fig. 6B, C, E, and Table 2). In addition, vBVD12$^-$ was also produced in the supernatant (Fig. 6B, D, E, and Table 2). The result of HiDi PCR shown in Fig. 6B shows that the vBVD12$^-$ gene was not detected at many passage points, which was likely to be related to the detection sensitivity of the HiDi PCR. In fact, this method cannot detect a viral gene unless it is present at $10^{4.0}$ TCID50 or more in 1 mL (data not shown). It is possible that low-titer vBVD12$^-$ was present at the passage point where the viral gene was not detected by HiDi PCR. Of note, co-infection with the END$^-$ virus allowed the END$^+$ virus to propagate under conditions wherein host immune response was activated. Thus, co-infection with the END$^-$ virus may be necessary to permit the evasion of host innate immune responses; this evasion would contributes to the maintenance of persistent infection both *in vitro* and *in vivo*. However, we could not clarify the mechanism via which the END$^-$ virus supports END$^+$ virus propagation. To unravel this mechanism, it will be necessary to estimate the genetic diversity of each virus in detail. For example, via viral gene mutation and recombination studies, we will need to investigate whether the END$^-$ or END$^+$ virus is likely to generate the END$^+$ or END$^-$ virus.

Our co-infection experiments conducted using cultured cells demonstrated that infection with the BVDV/END$^-$ can support the propagation of BVDV/END$^+$ in the presence of host innate immune responses. Co-infection with the END$^-$ virus contributes to the evasion of innate immunity, which may permit persistent infection of BVDV. Moreover, our results also strongly suggest that the END$^-$ virus, with previously unknown biological significance, acts as a helper virus and supports the propagation of other virus types. Further detailed characterization of the END$^-$ virus will help elucidate the pathogenesis and the complex immune regulatory mechanisms caused by BVDV.

4. Materials and methods

4.1. Cells and viruses

MDBK cells were cultured as a monolayer in Eagle's Minimum Essential Medium (MEM; Nissui, Tokyo, Japan) containing 0.295% tryptose phosphate broth, 1% inactivated anti-BVDV antibody-free fetal bovine serum (FBS; Japan Bio Serum, Hiroshima, Japan), 1% horse serum (Thermo Fisher Scientific, Rockford, IL), 1.125 mg/mL $NaHCO_3$, 2 mM L-glutamine, and antibiotics (100 IU/mL penicillin and 100 μg/mL streptomycin). Bovine testicle (BT) cells were prepared from a pestivirus-free animal and cultured in MEM containing 10% inactivated FBS, 1.125 mg/mL $NaHCO_3$, 2 mM L-glutamine, and antibiotics. The No.12 strain of ncpBVDV-1/ END$^+$ and the END$^-$ virus were prepared using virus cloning methods employing an END assay based on limiting dilution and RPF assay, respectively. NDV (Miyadera strain) and VSV (New Jersey strain) were used as challenge viruses. VSV was obtained from the National Institute of Animal Health (Tsukuba, Japan) under

approval from the Ministry of Agriculture, Forestry and Fishery, Japan. NDV was propagated in the allantoic cavities of 9-day-old embryonated hens' eggs. VSV was propagated in the Vero cell line.

4.2. Antibodies and reagents

Mouse monoclonal antibody (#46/1), raised against the pestivirus NS3 protein, was generated as described previously (Kameyama et al., 2006). Horseradish peroxidase-conjugated sheep antibody against mouse IgG (SurModics, Eden Prairie, MN) was used as the secondary antibody for PLA. Human recombinant IFN-α (Acris Antibodies GmbH, Herford, Germany) was adjusted to 10 ng/μL. Human type-I IFN neutralizing antibody mixture (PBL assay science, Piscataway, NJ) was used for neutralizing IFNs within the viral fluid. IFN neutralization was performed following the manufacturer's protocol.

4.3. Plasmids

PCR to amplify the complete BVDV genome was performed using cDNA synthesized from ncpBVDV-1 strain No. 12 END$^-$ viral RNA. A BVDV cDNA clone was inserted between the *Mlu*I and *Sma*I sites of a modified pA187-1 vector (Ruggli et al., 1996) using DNA ligation and In-Fusion cloning (Takara Bio, Shiga, Japan), and the resulting plasmid was designated pBVD12$^-$. The plasmid carrying the Pro8Leu substitution in the N^{pro}-encoding region (i.e., carrying a mutation at nucleotide 410) of pBVD12$^-$ was constructed using a Mutagenesis kit (Takara Bio) and appropriate oligonucleotide primers, and the resulting plasmid was designated pBVD12$^-$/P8L. The sequences of the plasmids used in the current study were confirmed by Eurofins Genomics (Tokyo, Japan). The nucleotide sequences were analyzed using GENETYX software (version 9.0.7; Genetyx, Tokyo, Japan).

4.4. Production of vBVD12$^-$ and vBVD12$^-$/P8L

The plasmids pBVD12$^-$ and pBVD12$^-$/P8L were digested with *Sma*I (near the 3′-end) and the resulting linearized plasmids were transcribed *in vitro* using either the MEGAscript T7 kit (Life Technologies, Grand Island, NY) or the T7 RiboMAX < SUP > TM < / SUP > Express Large Scale RNA Production System (Promega, Madison, WI) following manufacturers' instructions. MDBK cells (cell density, 5 × 10^6 cells' volume, 0.5 mL) were electroporated with the *in vitro* transcribed RNA (10 μg) using a 0.4-mm gap electroporation cuvette (NEPA GENE CO., LTD., Chiba, Japan). The electroporation conditions were 360–380 V for 10 ms and 20 V for 50 ms and 50 ms × 5 using a CUY21 Vitro-EX (BEX, Tokyo, Japan). The cells were allowed to recover in MEM containing 5% FBS. Post incubation for 3 days, the culture supernatants of vBVD12$^-$ or vBVD12$^-$/P8L were harvested as passage 0 (P.0). To increase the viral titers, the P.0 culture supernatants were subjected to further rounds of passaging in MDBK cells. It has been confirmed that neither vBVD12$^-$ nor vBVD12$^-$/P8L shows CPE in cultured cells.

4.5. IFN bioassay

The viral particles in each culture supernatant were eliminated using an Amicon Ultra 0.5-mL filter (Merck KGaA, Darmstadt, Germany). Each filtered supernatant (flow-through) was used as a sample for the IFN bioassay. Each sample was serially diluted two-fold, and 100 μL of each resulting dilution was added to the MDBK cell monolayer in each well of a 96-well culture plate (Figs. 1C and 6D). The filtered supernatant was used without dilution (Fig. 3B). The plates were then incubated at 37 °C under 5% CO_2 for 24 h. After supernatant removal, the cells were superinfected with VSV at an MOI of 2. After incubation for 2 days, a solution of 0.25% crystal violet in 10% methanol and 7.5% formalin was added to each well. OD values were measured at a wavelength of 595 nm using a Multiskan FC plate reader (Thermo Fisher Scientific). The bioassay was performed twice, and the average OD value for each sample was calculated. The sum of half of the negative (VSV-infected cells) and positive (mock-infected cells) control OD values was taken as the 50% OD value; samples that yielded a value higher than this value were inferred to contain IFN-α/β at levels sufficient to block the CPE of VSV by ≥ 50% (Ogiso et al., 2005).

4.6. Virus titration and peroxidase-linked assay (PLA)

The virus samples were serially diluted 10-fold, and 50 μL of each dilution was added to four wells of a 96-well microplate. MDBK cells (100 μL) were seeded at a density of approximately 2.5 × 10^4 cells/well. The plate was then incubated for 5 days. The infected cells were fixed at 75 °C for 60 min after washing once with phosphate-buffered saline (PBS) (−). The monoclonal antibody against the pestivirus NS3 protein was diluted in dilution buffer (0.05% Tween-20 and 1% bovine serum albumin in PBS) and then added (50 μL/well) to the fixed cells. The plates were then incubated at 37 °C for 60 min. After removal of the primary antibody, the cells were washed once with PBS (−). The secondary antibody was diluted in dilution buffer and added to the cells, and the plates were again incubated at 37 °C for 60 min. The cells were washed once with PBS (−), and substrate buffer (5 mM acetate buffer, 3-amino-9-ethylcarbazole [Sigma-Aldrich, St. Louis, MO] solution, 30% H_2O_2 [FUJIFILM Wako Pure Chemical Corporation, Osaka, Japan]) was then added to each well. Successful reaction between the enzyme and substrate was indicated by red staining in the cytoplasm of BVDV-positive cells. The TCID50 was calculated following the method described by Kärber (1931). The titration was performed thrice, and the average value was calculated as the viral titer. The virus detection sensitivities of the END and RPF assays has been confirmed to be equivalent to that of PLA (data not shown).

4.7. END assay

The END assay, which was used for END$^+$ virus titrations, was performed following the original method (Inaba et al., 1963). If the supernatant sample contained exogenous IFN-α, it was eliminated by filtration prior to infection experiments. Briefly, after each 10-fold serial dilution of BVDV, 50 μL of each dilution was added to four wells of a 96-well microplate. Cells were added to the wells by distributing MDBK cell at 0.1 mL (approximately 2.0 × 10^4 cells) per well. The plate then was incubated for 5 days before aspiration of culture fluid from each well. Then, 100 μL of NDV suspension (10$^{7.0}$ TCID50/mL) was added to each well and the plate was incubated for another 2 days. The cells were examined for CPE using a light microscope; cells were considered BVDV/END$^+$-positive if CPE was enhanced. The viral titer was estimated based on the highest dilution of END$^+$ yielding CPE upon NDV superinfection (limiting dilution). The TCID50 was calculated following the method described by Kärber (1931). Titration of END$^+$ viruses was performed thrice, and the average value was calculated as the viral titer. When the END assay was used to confirm the biological properties of BVDV, MDBK cells grown in six-well plates were infected with appropriate viral samples and incubated for 4–5 days. After supernatant removal, the cells were superinfected with 1 mL of an NDV suspension (10$^{6.0}$ TCID50/mL), and the plate was incubated for another 1–2 days prior to evaluation.

4.8. VSV interference assay

The VSV interference assay was performed following the method described by Fukusho et al. (1975); however, MDBK cells were used. In case the supernatant sample contained exogenous IFN-α, it was eliminated by filtration and then used for infection experiments. In brief, MDBK cells grown in six-well plates were infected with the indicated virus samples and incubated for 4–5 days. After supernatant removal, the cells were superinfected with VSV at an MOI of 2. The sample was

regarded as BVDV/END$^-$-positive for VSV interference if no CPE was observed upon VSV superinfection in BVDV-infected cells.

4.9. RPF assay

The RPF assay was performed following the original method by Fukusho et al. (1976), but with slight modifications. In case the supernatant sample contained exogenous IFN-α, it was eliminated by filtration and then used for infection experiments. The virus samples were serially diluted 10-fold with MEM prior to inoculating each well of the six-well plates containing confluent monolayers of BT cells. The plates were incubated at 37 °C under 5% CO_2 for virus absorption. After 90 min, the wells were washed with PBS (−) and the contents of each well were overlaid with approximately 5 mL of methylcellulose overlay medium (MEM containing 7% FBS and 3% methylcellulose). After incubation for 5 days, the overlay medium was removed and the wells were washed with warm PBS (−). The infected cell monolayer was challenged with VSV at an MOI of 2, and the plates were then incubated for 60 min at 37 °C for absorption. The monolayer was washed with PBS (−) and again covered with methylcellulose overlay medium. After incubation for 2 days, the cells were fixed with methanol and stained with 0.25% crystal violet. Staining of reverse plaques indicated the presence of cells infected with the END$^-$ virus. For END$^-$ virus titer measurements, the RPF assay was performed thrice, and the average value was taken as the viral titer. The titer calculated by the RPF method (PFU/mL) was then converted into TCID50/mL.

4.10. Quantitative reverse transcription PCR (qRT-PCR)

MDBK cells were treated with the appropriate supernatant samples (or virus produced by reverse genetics) and incubated for 12 or 24 h. For quantification of bovine *Mx1* and *ISG15* mRNAs, total RNA was extracted from the cells using the RealTime ready Cell Lysis Kit (Roche, Mannheim, Germany). First-strand cDNA synthesis was performed using the Transcriptor Universal cDNA Master Kit (Roche) following the manufacturer's instructions. qRT-PCR was performed using the PowerUP SYBR Green PCR Master Mix (Thermo Fisher Scientific) following the manufacturer's instructions. Fluorescent signals were detected using the StepOnePlus < SUP > TM < /SUP > Real-time PCR system (Thermo Fisher Scientific). The expression level of each mRNA was normalized to the amount of *GAPDH* mRNA in each sample and quantified using gene-specific primers as described previously (Yamane et al., 2008; Liu et al., 2009). Calculations were performed using the ΔΔCt method.

4.11. Conventional PCR and PCR with HiDi DNA polymerase

Conventional PCR, performed to amplify the N^{pro}-encoding region, was conducted using PrimeSTAR GXL DNA polymerase (TaKaRa Bio) (forward primer: 5′-AGGGCATGCCCAAAGCACATCTT-3′; reverse primer, 5′-CCTGGTATTTGACTCCATCTACCACTAT-3′). These primers were used to amplify an 802-bp fragment of the BVDV genome extending from the 5′-untranslated region (UTR) through the region encoding N^{pro}. The PCR conditions were as follows: 1 cycle at 94 °C for 1 min followed by 35 cycles at 98 °C for 10 s, 55 °C for 15 s, and 68 °C for 1 min. HiDi DNA polymerase (myPOLS Biotec GmbH, Konstanz, Germany) efficiently amplifies sequences from primers that match the template at the 3′-end of the primer, discriminating primers that are mismatched to the template. Because vBVD12$^-$ and vBVD12$^-$/P8L differ only by a one-base mutation in the region encoding N^{pro} (at nucleotide 410), it is possible to discriminate the sequences of the respective viruses using HiDi DNA polymerase. The templates used for PCR were cDNAs reverse transcribed from total RNA extracted from the culture supernatant samples. Total RNA extraction and cDNA synthesis were performed using the TRIzol LS Reagent (Thermo Fisher Scientific) and the PrimeScript RT-PCR Kit (TaKaRa Bio), respectively, following the respective manufacturers' instructions. Total RNA was extracted from a quantity of viruses with their titers adjusted to $10^{5.0}$ TCID50/mL. Specific primers were designed following the HiDi DNA polymerase manufacturer's recommendations. For the amplification of the desired region of the N^{pro}-encoding gene from vBVD12$^-$ or vBVD12$^-$/P8L, PCR was performed using the forward primers 5′-ACATGGAGTTGATT ACAAATGAACC-3′ or 5′-ACATGGAGTTGATTACAAATGAACT-3′, respectively, in combination with the universal reverse primer 5′-TCGT TTTGGTAAAGAAGCCAAATTG-3′. These primer pairs were expected to amplify a 200-bp fragment of the BVDV genome extending from the 5′-UTR through the region encoding N^{pro}. The PCR conditions for the amplification of the vBVD12$^-$ sequence were as follows: 1 cycle at 95 °C for 2 min followed by 27 cycles at 95 °C for 15 s, 55 °C for 10 s, and 72 °C for 30 s. The PCR conditions for the amplification of the vBVD12$^-$/P8L sequences were as follows: 1 cycle at 95 °C for 2 min followed by 35 cycles at 95 °C for 15 s, 54 °C for 10 s, and 72 °C for 30 s. The PCR products were electrophoresed on 2% agarose gels, stained with ethidium bromide, and visualized under ultraviolet light.

4.12. Virus passage

Culture flasks (surface area, 25 cm^2) were used for supernatant passaging.

4.12.1. Supernatant passaging during infection with a single virus (Fig. 2, left and middle panels)

MDBK cells were separately infected with either vBVD12$^-$ or vBVD12$^-$/P8L at an MOI of 1 at the time of cell seeding; the cultures were then incubated for 4 days. After incubation, the culture supernatant was collected and centrifuged at 400 × *g* for 10 min at 4 °C to remove debris. An aliquot of the culture supernatant was stored at −80 °C. Approximately 3 × 10^5 naïve MDBK cells were inoculated with 0.5 mL of the supernatant at the time of cell seeding; the cultures were then incubated for 4 days. This passaging procedure was repeated 10 times, and the culture supernatant collected at each step was designated as P.1–P.10.

4.12.2. Supernatant passaging during co-infection studies (Fig. 2, right panel)

MDBK cells were infected with both vBVD12$^-$ and vBVD12$^-$/P8L at an MOI of 1. The culture supernatant was passaged following the protocol for passaging following infection with a single virus.

4.12.3. Supernatant passaging during infection with a single virus with addition of exogenous IFN-α (Fig. 5A and E)

MDBK cells were seeded in flasks and separately infected with viruses at an MOI of 0.1; the flasks were then incubated for 60 min to allow virus absorption. The inoculum was removed and replaced with 5 mL of fresh medium containing 3 ng (P.1–P.7) or 30 ng (P.8–P.25) of IFN-α; the flasks were then incubated for 4–5 days. After incubation, the culture supernatants were collected and centrifuged at 400 × *g* for 10 min at 4 °C. A 1 mL-aliquot of the supernatant was inoculated onto a monolayer of MDBK cells in a flask; the flask was then incubated for 60 min. The inoculum was removed and replaced with 5 mL of fresh medium containing IFN-α. This passaging procedure was repeated until P.25 was reached.

4.12.4. Supernatant passaging during co-infection studies with addition of exogenous IFN-α (Fig. 6A)

MDBK cells were seeded in flasks and then infected with BVDVs at an MOI of 0.1. The cultures were incubated for 60 min to allow virus absorption. Passaging of the supernatant and addition of IFN-α were performed in the manner described above for supernatant passaging during infection with a single virus with addition of exogenous IFN-α.

4.13. Deep sequencing and genome analysis

The supernatants were collected and stored at −80 °C until further analysis. Viral RNA was extracted from the culture supernatants using the TRIzol LS Reagent (Thermo Fisher SCIENTIFIC) and subsequently treated with DNase I (Takara Bio). For deep sequencing, cDNA libraries were constructed using the NEBNext Ultra RNA Library Prep Kit for Illumina (New England Biolabs, Ipswich, MA), as described previously (Nagai et al., 2015). Deep sequencing was conducted using the MiSeq Reagent Kit v2 (300 cycles; Illumina, San Diego, CA) on a MiSeq benchtop sequencer (Illumina). The sequence data were analyzed using CLC Genomics Workbench 6.5.1 (Qiagen). Raw reads were trimmed according to sequence quality, and variant detection was performed using the quality-based variant detection command. Contigs were generated from trimmed sequence reads with default parameter setting in CLC Genomics Workbench.

4.14. Statistical analysis

The averages of three independent experiments were taken as the data for statistical analyses. Results were expressed as means ± standard deviations. The significance of the differences between group means was determined using unpaired or paired Student's *t*-tests.

Declaration of competing interest

The authors declare that they have no known competing financial interests or personal relationships that could have appeared to influence the work reported in this paper.

Acknowledgements

We would like to thank Yuri Abe and Dr. Masatoshi Okamatsu (Hokkaido University, Japan) for support with construction of pBVD12$^-$ and pBVD12$^-$/P8L and production of viruses derived from these plasmids.

We would like to thank Ayano Kato for contributing to the establishment of reverse genetics methods of ncpBVDV-1 No.12 strain.

Appendix A. Supplementary data

Supplementary data to this article can be found online at https://doi.org/10.1016/j.virol.2019.09.016.

Funding

This work was supported by JSPS KAKENHI Grant in Aid for Young Scientists B Number 16K18796.

References

Aoki, H., Sakoda, Y., Nakamura, S., Suzuki, S., Fukusho, A., 2004. Cytopathogenicity of classical swine fever viruses that do not show the exaltation of Newcastle disease virus is associated with accumulation of NS3 in serum-free cultured cell lines. J. Vet. Med. Sci. 66, 161–167. https://doi.org/10.1292/jvms.66.161.

Baigent, S.J., Zhang, G., Fray, M.D., Goodbourn, S., Mccauley, J.W., Flick-smith, H., 2002. Inhibition of beta interferon transcription by noncytopathogenic bovine viral diarrhea virus is through an interferon regulatory factor 3-dependent mechanism. J. Virol. 76, 8979–8988. https://doi.org/10.1128/JVI.76.18.8979.

Brackenbury, L.S., Carr, B.V., Stamataki, Z., Prentice, H., Lefevre, E.A., Howard, C.J., Charleston, B., 2005. Identification of a cell population that produces alpha/beta interferon in vitro and in vivo in response to noncytopathic bovine viral diarrhea virus. J. Virol. 79, 7738–7744. https://doi.org/10.1128/JVI.79.12.7738-7744.2005.

Brownlie, J., 1990. Pathogenesis of mucosal disease and molecular aspects of bovine virus diarrhoea virus. Vet. Microbiol. 23, 371–382. https://doi.org/10.1016/0378-1135(90)90169-V.

Charleston, B., Fray, M.D., Baigent, S., Carr, B.V., Morrison, W.I., 2001. Establishment of persistent infection with non-cytopathic bovine viral diarrhoea virus in cattle is associated with a failure to induce type I interferon. J. Gen. Virol. 82, 1893–1897. https://doi.org/10.1099/0022-1317-82-8-1893.

Durantel, D., Carrouée-Durantel, S., Branza-Nichita, N., Dwek, R.A., Zitzmann, N., 2004. Effects of interferon, ribavirin, and iminosugar derivatives on cells persistently infected with noncytopathic bovine viral diarrhea virus. Antimicrob. Agents Chemother. 48, 497–504. https://doi.org/10.1128/AAC.48.2.497-504.2004.

Fourichon, C., Beaudeau, F., Bareille, N., Seegers, H., 2005. Quantification of economic losses consecutive to infection of a dairy herd with bovine viral diarrhoea virus. Prev. Vet. Med. 72, 177–181. https://doi.org/10.1016/j.prevetmed.2005.08.018.

Fukusho, A., Ogawa, N., Yamamoto, H., Iwata, Y., Sawada, M., Sazawa, H., 1975. Interference method with vesicular stomatitis virus for detection of GPE$^-$ strain of hog cholera virus. Annu. Rep. Natl. Vet. Assay Lab. 12, 9–14.

Fukusho, A., Ogawa, N., Yamamoto, H., Sawada, M., Sazawa, H., 1976. Reverse plaque formation by hog cholera virus of the GPE$^-$ strain inducing heterologous interference. Infect. Immun. 14, 332–336.

Gil, G., Ansari, I.H., Vassilev, V., Liang, D., Lai, V.C.H., Zhong, W., Hong, Z., Dubovi, E.J., Donis, R.O., 2006. The amino-terminal domain of bovine viral diarrhea virus N^{pro} protein is necessary for alpha/beta interferon antagonism. J. Virol. 80, 900–911. https://doi.org/10.1128/JVI.80.2.900.

Gottipati, K., Holthauzen, L.M.F., Ruggli, N., Choi, K.H., 2016. Pestivirus N^{pro} directly interacts with interferon regulatory factor 3 (IRF3) monomer and dimer. J. Virol. 90, 7740–7747. https://doi.org/10.1128/JVI.00318-16.

Harding, M.J., Cao, X., Shams, H., Johnson, A.F., Vassilev, V.B., Gil, L.H., Wheeler, D.W., Haines, D., Sibert, G.J., Nelson, L.D., Campos, M., Donis, R.O., 2002. Role of bovine viral diarrhea virus biotype in the establishment of fetal infections. Am. J. Vet. Res. 63, 1455–1463. https://doi.org/10.2460/ajvr.2002.63.1455.

Hilton, L., Moganeradj, K., Zhang, G., Chen, Y.-H., Randall, R.E., McCauley, J.W., Goodbourn, S., 2006. The NPro product of bovine viral diarrhea virus inhibits DNA binding by interferon regulatory factor 3 and targets it for proteasomal degradation. J. Virol. 80, 11723–11732. https://doi.org/10.1128/JVI.01145-06.

Inaba, Y., Omori, T., Kumagai, T., 1963. Detection and measurement of non-cytopathogenic strains of virus diarrhea of cattle by the END method. Arch. Gesamte Virusforsch. 13, 425–429. https://doi.org/10.1007/BF01244615.

Inaba, Y., Tanaka, Y., Kumagai, T., Omori, T., Ito, H., Matumoto, M., 1968. Bovine diarrhea virus II. END Phenomenon : exaltation of Newcastle disease virus in bovine cells infected with bovine diarrhea virus. Jpn. J. Microbiol. 12, 35–49.

Itoh, O., Sugiyama, M., Nakamura, S., Sasaki, H., 1984. Characterization of a non-cytopathogenic agent isolated from cytopathogenic bovine viral diarrhea-mucosal disease virus stock. Microbiol. Immunol. 28, 1163–1167.

Kameyama, K., Sakoda, Y., Tamai, K., Igarashi, H., Tajima, M., Mochizuki, T., Namba, Y., Kida, H., 2006. Development of an immunochromatographic test kit for rapid detection of bovine viral diarrhea virus antigen. J. Virol. Methods 138, 140–146. https://doi.org/10.1016/j.jviromet.2006.08.005.

Kärber, G., 1931. Beitrag zur kollektiven Behandlung pharmakologischer Reihenversuche. Naunyn Schmiedebergs. Arch. Pharmacol. 162, 480–483. https://doi.org/10.1007/BF01863914.

Kozasa, T., Abe, Y., Mitsuhashi, K., Tamura, T., Aoki, H., Ishimaru, M., Nakamura, S., Okamatsu, M., Kida, H., Sakoda, Y., 2015. Analysis of a pair of END$^+$ and END$^-$ viruses derived from the same bovine viral diarrhea virus stock reveals the amino acid determinants in N^{pro} responsible for inhibition of type I interferon. J. Vet. Med. Sci. 77, 511–518. https://doi.org/10.1292/jvms.14-0420.

Kumagai, T., Shimizu, T., Matumoto, M., 1958. Detection of hog cholera virus by its effect on Newcastle disease virus in swine culture. Science 128 (3320), 366. https://doi.org/10.1126/science.128.3320.366.

Lanyon, S.R., Hill, F.I., Reichel, M.P., Brownlie, J., 2014. Bovine viral diarrhoea: pathogenesis and diagnosis. Vet. J. 199, 201–209. https://doi.org/10.1016/j.tvjl.2013.07.024.

Liu, C., Chang, R., Yao, X., Qiao, W.T., Geng, Y.Q., 2009. ISG15 expression in response to double-stranded RNA or LPS in cultured Fetal Bovine Lung (FBL) cells. Vet. Res. Commun. 33, 723–733. https://doi.org/10.1007/s11259-009-9221-8.

Magkouras, I., Mätzener, P., Rümenapf, T., Peterhans, E., Schweizer, M., 2008. RNase-dependent inhibition of extracellular, but not intracellular, dsRNA-induced interferon synthesis by E^{rns} of pestiviruses. J. Gen. Virol. 89, 2501–2506. https://doi.org/10.1099/vir.0.2008/003749-0.

Meyers, G., Ege, A., Fetzer, C., von Freyburg, M., Elbers, K., Carr, V., Prentice, H., Charleston, B., Schurmann, E.-M., 2007. Bovine viral diarrhea virus: prevention of persistent fetal infection by a combination of two mutations affecting E^{rns} RNase and N^{pro} protease. J. Virol. 81, 3327–3338. https://doi.org/10.1128/JVI.02372-06.

Mine, J., Tamura, T., Mitsuhashi, K., Okamatsu, M., Parchariyanon, S., Pinyochon, W., Ruggli, N., Tratschin, J.-D., Kida, H., Sakoda, Y., 2015. The N-terminal domain of N^{pro} of classical swine fever virus determines its stability and regulates type I IFN production. J. Gen. Virol. 96, 1746–1756. https://doi.org/10.1099/vir.0.000132.

Nagai, M., Omatsu, T., Aoki, H., Otomaru, K., Uto, T., Koizumi, M., Minami-Fukuda, F., Takai, H., Murakami, T., Masuda, T., Yamasato, H., Shiokawa, M., Tsuchiaka, S., Naoi, Y., Sano, K., Okazaki, S., Katayama, Y., Oba, M., Furuya, T., Shirai, J., Mizutani, T., 2015. Full genome analysis of bovine astrovirus from fecal samples of cattle in Japan: identification of possible interspecies transmission of bovine astrovirus. Arch. Virol. 160, 2491–2501. https://doi.org/10.1007/s00705-015-2543-7.

Nakamura, S., Fukusho, A., Inoue, Y., Sasaki, H., Ogawa, N., 1993. Isolation of different non-cytopathogenic bovine viral diarrhoea (BVD) viruses from cytopathogenic BVD virus stocks using reverse plaque formation method. Vet. Microbiol. 38, 173–179. https://doi.org/10.1016/0378-1135(93)90084-K.

Nakamura, S., Shimazaki, T., Sakamoto, K., Fukusho, A., Inoue, Y., Ogawa, N., 1995. Enhanced replication of orbiviruses in bovine testicle cells infected with bovine viral diarrhoea virus. J. Vet. Med. Sci. 57, 677–681. http://doi.org/10.1292/jvms.57.677.

Nishine, K., Aoki, H., Sakoda, Y., Fukusho, A., 2014. Field distribution of END phenomenon-negative bovine viral diarrhea virus. J. Vet. Med. Sci. 76, 1635–1639. https://doi.org/10.1292/jvms.14-0220.

Ogiso, S., Shirai, J., Tuchiya, Y., Honda, E., 2005. Use of Getah virus for antiviral assay of human interferon. Uirusu 55, 317–326. https://doi.org/10.2222/jsv.55.317.

Peek, S.F., Bonds, M.D., Schaele, P., Weber, S., Friedrichs, K., Schultz, R.D., 2004. Evaluation of antiviral activity and toxicity of recombinant human interferon alfa-2a in calves persistently infected with type 1 bovine viral diarrhea virus. Am. J. Vet. Res. 65, 865–870.

Peterhans, E., Schweizer, M., 2013. BVDV: a pestivirus inducing tolerance of the innate immune response. Biologicals 41, 39–51. https://doi.org/10.1016/j.biologicals.2012.07.006.

Reid, E., Juleff, N., Windsor, M., Gubbins, S., Roberts, L., Morgan, S., Meyers, G., Perez-Martin, E., Tchilian, E., Charleston, B., Seago, J., 2016. Type I and III IFNs produced by plasmacytoid dendritic cells in response to a member of the Flaviviridae suppress cellular immune responses. J. Immunol. 196, 4214–4226. https://doi.org/10.4049/jimmunol.1600049.

Richter, V., Lebl, K., Baumgartner, W., Obritzhauser, W., Käsbohrer, A., Pinior, B., 2017. A systematic worldwide review of the direct monetary losses in cattle due to bovine viral diarrhoea virus infection. Vet. J. 220, 80–87. https://doi.org/10.1016/j.tvjl.2017.01.005.

Ruggli, N., Tratschin, J.D., Mittelholzer, C., Hofmann, M.A., 1996. Nucleotide sequence of classical swine fever virus strain Alfort/187 and transcription of infectious RNA from stably cloned full-length cDNA. J. Virol. 70, 3478–3487.

Ruggli, N., Tratschin, J.D., Schweizer, M., Mccullough, K.C., Hofmann, M.A., Summerfield, A., 2003. Classical swine fever virus interferes with cellular antiviral defense: evidence for a novel function of N^{pro}. J. Virol. 77, 7645–7654. https://doi.org/10.1128/JVI.77.13.7645.

Schweizer, M., Peterhans, E., 2001. Noncytopathic bovine viral diarrhea virus inhibits double-stranded RNA-induced apoptosis and interferon synthesis. J. Virol. 75, 4692–4698. https://doi.org/10.1128/JVI.75.10.4692.

Schweizer, M., Matzener, P., Pfaffen, G., Stalder, H., Peterhans, E., 2006. "Self" and "nonself" manipulation of interferon defense during persistent infection: bovine viral diarrhea virus resists alpha/beta interferon without blocking antiviral activity against unrelated viruses replicating in its host cells. J. Virol. 80, 6926–6935. https://doi.org/10.1128/JVI.02443-05.

Seago, J., Hilton, L., Reid, E., Doceul, V., Jeyatheesan, J., Moganeradj, K., McCauley, J., Charleston, B., Goodbourn, S., 2007. The N^{pro} product of classical swine fever virus and bovine viral diarrhea virus uses a conserved mechanism to target interferon regulatory factor-3. J. Gen. Virol. 88, 3002–3006. https://doi.org/10.1099/vir.0.82934-0.

Shimizu, Y., Furuuchi, S., Kumagai, T., Sasahara, J., 1970. A mutant of hog cholera virus inducing interference in swine testicle cell cultures. Am. J. Vet. Res. 31, 1787–1794.

Shoemaker, M.L., Smirnova, N.P., Bielefeldt-Ohmann, H., Austin, K.J., van Olphen, A., Clapper, J.A., Hansen, T.R., 2009. Differential expression of the type I interferon pathway during persistent and transient bovine viral diarrhea virus infection. J. Interferon Cytokine Res. 29, 23–36. https://doi.org/10.1089/jir.2008.0033.

Smirnova, N.P., Webb, B.T., Bielefeldt-Ohmann, H., Van Campen, H., Antoniazzi, A.Q., Morarie, S.E., Hansen, T.R., 2012. Development of fetal and placental innate immune responses during establishment of persistent infection with bovine viral diarrhea virus. Virus Res. 167, 329–336. https://doi.org/10.1016/j.virusres.2012.05.018.

Smirnova, N.P., Webb, B.T., McGill, J.L., Schaut, R.G., Bielefeldt-Ohmann, H., Van Campen, H., Sacco, R.E., Hansen, T.R., 2014. Induction of interferon-gamma and downstream pathways during establishment of fetal persistent infection with bovine viral diarrhea virus. Virus Res. 183, 95–106. https://doi.org/10.1016/j.virusres.2014.02.002.

Tamura, T., Nagashima, N., Ruggli, N., Summerfield, A., Kida, H., Sakoda, Y., 2014. N^{pro} of classical swine fever virus contributes to pathogenicity in pigs by preventing type I interferon induction at local replication sites. Vet. Res. 45. https://doi.org/10.1186/1297-9716-45-47.

Tratschin, J.D., Moser, C., Ruggli, N., Hofmann, M.A., 1998. Classical swine fever virus leader proteinase N^{pro} is not required for viral replication in cell culture. J. Virol. 72, 7681–7684.

Van Wyk, B., Snider, M., Scruten, E., van Drunen Littel-van den Hurk, S., Napper, S., 2016. Induction of functional interferon alpha and gamma responses during acute infection of cattle with non-cytopathic bovine viral diarrhea virus. Vet. Microbiol. 195, 104–114. https://doi.org/10.1016/j.vetmic.2016.09.015.

Yamane, D., Kato, K., Tohya, Y., Akashi, H., 2008. The relationship between the viral RNA level and upregulation of innate immunity in spleen of cattle persistently infected with bovine viral diarrhea virus. Vet. Microbiol. 129, 69–79. https://doi.org/10.1016/j.vetmic.2007.11.004.

Zhang, G., Aldridge, S., Clarke, M.C., McCauley, J.W., 1996. Cell death induced by cytopathic bovine viral diarrhoea virus is mediated by apoptosis. J. Gen. Virol. 77, 1677–1681. https://doi.org/10.1099/0022-1317-77-8-1677.

Zurcher, C., Sauter, K.-S., Mathys, V., Wyss, F., Schweizer, M., 2014. Prolonged activity of the pestiviral RNase E^{rns} as an interferon antagonist after uptake by clathrin-mediated endocytosis. J. Virol. 88, 7235–7243. https://doi.org/10.1128/JVI.00672-14.